Progress In Electromagnetics Research, PIER 83, 1–11, 2008

A NOVEL DUAL BAND TRANSMITTER USING MICROSTRIP DEFECTED GROUND STRUCTURE

X. Q. Chen, X. W. Shi, Y. C. Guo, and C. M. Xiao

State Key Lab. of Antennas and Microwave Technology
Xidian University
Xi'an 710071, P. R. China

Abstract—This paper presented a novel dual band transmitter which operates as power amplifier or frequency doubler with the stop band characteristic of defected ground structure (DGS). It works as a power amplifier at 2.4 GHz which satisfies the 802.11b/g wireless LAN standard or performs as an active frequency doubler at 6.8 GHz which depends on the input frequency and. The equivalent circuit and the stop band characteristic of the proposed microstrip DGS are analyzed and simulated. For the proposed transmitter, second harmonic suppression is below −52.6 dBc in the amplifier mode, and fundamental suppression is below −41 dBc in the frequency doubler mode with the stop band characteristic of DGS. The designed transmitter used GaAs InGaP Heterojunction broadband MMIC. It achieves 13.7 dBm of $P_{1\,dB}$ and its gain is 16.5 dB in amplifier mode, and its maximum output power is 7.8 dBm at 6.8 GHz in frequency double mode.

1. INTRODUCTION

High speed wireless LAN technology is crucial in modern communication system and it propagates rapidly in the infrastructure of office and home environments. In 2002, the IEEE extended the 802.11b standard to higher data rates up to 54 Mbps by using the OFDM modulation of the 802.1la standard in the 2.4 GHz band [1]. And 802.1lg standard which is compatible to 802.11b and offers 54 Mb/s data rate was proposed by IEEE in 2003 to suffice the requirements [2, 3]. The continual growth of wireless LANs is being driven by the need to lower the costs associated with system and simplify the composition of devices.

For the wireless LAN application, dual band capability is necessary for compatibility and covering both of the standards [4]. There have been some presentations of the dual band transceiver

and they have used two separate RF modules at each band [5]. However, the difficulty to achieve satisfactory performance in the RF hardware over wide bandwidths drives designers toward architectures that incorporate dual-band transceiver architectures which switch their signal paths for different bands in different working situation. In RF front-end for wireless LAN, especially the power amplifier is one of key components which occupies relatively large portion of assembly area and cost. For the practical implementation of IEEE 802.11b/g RF front-end solution in dual band environments, the PA modules not only need to meet the required system performance, but also they need to be low cost and small compact size [6]. In this paper, the dual band transmitter design technique for 2.4 GHz and 6.8 GHz wireless LAN transmitter is presented.

The proposed dual band transmitter works as a power amplifier which satisfies the 802.11b/g frequency band of wireless LAN standard, and it also performs as a frequency doubler with the stop band characteristics of DGS according to the input frequency and bias. Compared with a conventional dual band wireless LAN transmitter, the proposed dual band module operates as an amplifier for the 802.11b/g signal and as a frequency doubler according to signal frequency which shows well performance in experiment results. The equivalent circuit and the stop band characteristic of the microstrip DGS are analyzed and simulated.

2. DUAL BAND TRANSMITTER

In active circuits, harmonic components could be generated from nonlinear semiconductor devices such as Schottky-barrier diodes, varactor diodes, step-recovery diodes (SRDs), and transistors. For active frequency multipliers and amplifier, controlling the conduction angle of the signal carrier by the input dc-bias voltage is the main source of harmonic signal generation [7]. As active devices, especially for dual band transmitter the frequency doubler operating at the second harmonic and the power amplifier at the fundamental frequency, the optimum impedances for the maximum powers at both bands and are different. Several factors such as harmonic suppression, impedances matching, bandwidth and insertion loss should be taken into consideration.

2.1. DGS Characteristics and Frequency Doubler Design

The dual band transmitter using microstrip line DGS which works at 2.4 GHz and 6.8 GHz wireless LAN applications is shown in Fig. 1.

It consists of a filter, power gain controller (PGC), voltage controlled oscillator (VCO) operating from 2.4 GHz to 3.4 GHz and the amplifier/ frequency doubler module for dual band transmitter. As most conventional dual band transmitter of the wireless LAN system used two separate RF modules for both bands, it also requires a power amplifier at each band [7]. Those structures usually require different a voltage controlled oscillator (VCO) for each band. And the VCO should works in very broad bandwidth.

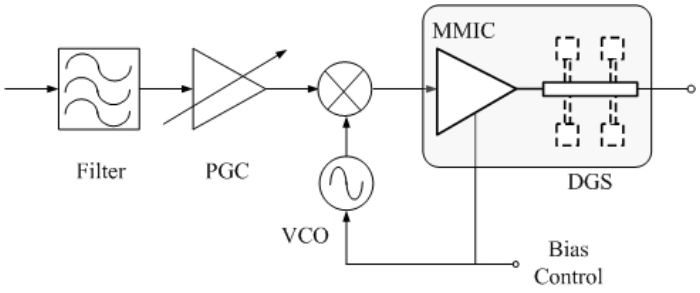

Figure 1. The proposed dual band transmitter with DGS block diagram.

In operating frequency of the dual band module, there are several frequency bands that should be suppressed, such as the fundamental frequency in the frequency doubler mode and the second harmonic in the amplifier mode. Usually fundamental frequency in the frequency doubler is suppressed by the $\lambda/4$ reflector, so the frequency doubler can generate more second harmonic. And the second harmonic in the amplifier can be suppressed by the $\lambda/4$ output bias line.

Here DGS circuit was used due to a number of attractive features. First, the DGS structure is very simple and it is easily simulated or fabricated and this is suitable for periodic structures design [8, 9]. They have been presented in a number of different shapes for filter applications [10–12]. Second, its stop band characteristic could be used to suppress certain harmonics. And the amplifier could improve its efficiency by the harmonics suppression and reduce size due to its slow wave effect [13]. Third, its insertion loss is much lower [14, 15]. Extremely small insertion loss values for implementation of RF circuits can be realized. The validity of the modeling method for the proposed DGS unit section and the design method is verified by experiments [16–18]. The DGS applied to a microstrip line causes a resonant character of the structure transmission with a resonant frequency controllable by changing the shape and size of the slot [19]. Fig. 2 and Fig. 3 show the proposed DGS structure and its equivalent circuit.

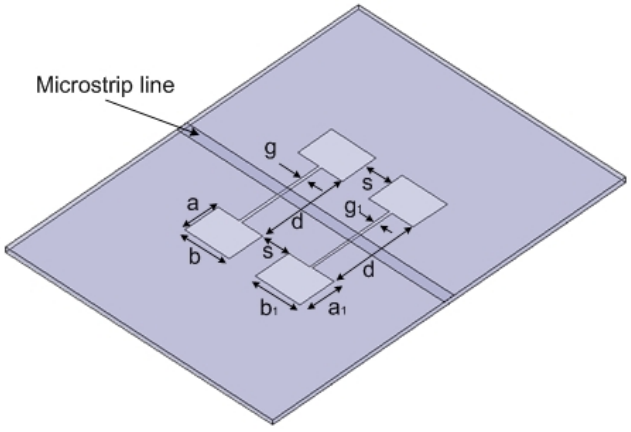

Figure 2. Proposed DGS on the ground plane.

In this paper, an asymmetric dumbbell module was proposed. The dimensions of the dumbbell are the following: $a = 3.8\,\text{mm}$, $b = 5\,\text{mm}$, $s = 4\,\text{mm}$, $d = 9\,\text{mm}$, $g = 0.3\,\text{mm}$, $a_1 = 3.9\,\text{mm}$, $b_1 = 5.2\,\text{mm}$, $g_1 = 0.28\,\text{mm}$. The equivalent circuit model with two LCR-network resonators for the proposed DGS model is shown in Fig. 3.

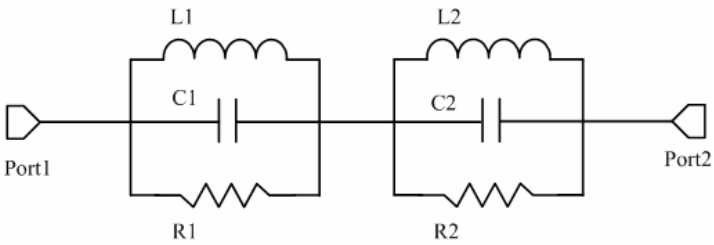

Figure 3. Equivalent circuit models of DGS.

The resonant characteristics are modeled by a LC-resonator, and the radiation effect and loss are considered by including resistor, R. Based on the transmission line theory and the spectral domain approach, the equivalent circuit parameters can be expressed using the following equations:

$$R(\omega) = \frac{2Z_0}{\sqrt{\dfrac{1}{|S_{11}(\omega)|^2} - \left(2Z_0\left(\omega C - \dfrac{1}{\omega L}\right)\right)^2} - 1} \tag{1}$$

$$C = \frac{\omega_c}{2Z_0\left(\omega_0^2 - \omega_c^2\right)} \tag{2}$$

$$L = \frac{1}{4(\pi f_0)^2 C} \tag{3}$$

where Z_0 is the 50 Ω characteristic impedance of the transmission line, f_0 is the resonant frequency, and Δf is the −3 dB bandwidth of S_{21}.

The stopband characteristic of DGS with different distance d which is the length between two rectangular lattices was shown in Fig. 4. When d decreases from 10 mm to 8 mm, the attenuation poles move to higher frequency from 3.2 GHz to 3.6 GHz. Usually, the DGS is fabricated to have a wide stopband bandwidth. Here the proposed DGS is designed to achieve the stopband bandwidth which could satisfy the demands of the dual band transmitter from 3.4 GHz to 4.8 GHz.

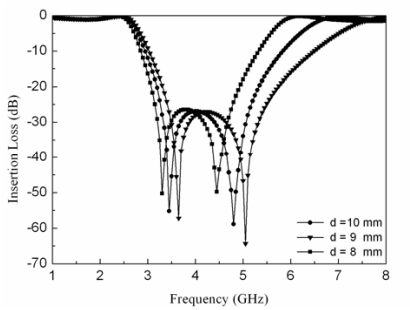

Figure 4. Comparison of stopband characteristic of DGS with different d.

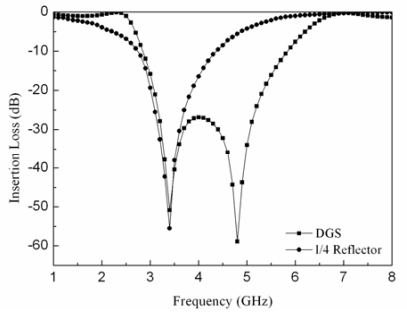

Figure 5. Stopband characteristic of DGS and $\lambda/4$ reflector.

The dual band module uses microstrip DGS in order to replace the $\lambda/4$ reflector by better stopband characteristic to suppress the fundamental power of the frequency doubler as well as the second harmonic of the amplifier. As it is known, the stopband bandwidth and attenuation degree of $\lambda/4$ reflector are decided by its width. If width of line is narrow, attenuation is good while its bandwidth is narrow. Also, if there are two separate bands needed to be suppressed, two $\lambda/4$ reflectors should be used. In this paper, we proposed the stopband characteristics between 3.4 GHz and 4.8 GHz, which used the microstrip DGS and its characteristic is shown in Fig. 5. The microstrip DGS is designed to suppress 3.4 GHz frequency band and 4.8 GHz frequency band while the $\lambda/4$ reflector only performs well at 3.4 GHz.

2.2. Power Amplifier Design

The proposed power amplifier works at 2.4 GHz for 802.11b/g is the other mode of the dual transmitter. The designed dual band circuit based on small signal has been analyzed by large signal with tuning of broadband matching circuits in order to accomplish power gain, linearity and maximum power [20]. So when the module operates as the amplifier, the second and third harmonic to the fundamental power at input frequency of 2.4 GHz are suppressed by the stopband characteristics of DGS. The input matching circuit is constructed to transmit the input frequency of 2.4 GHz to 3.4 GHz, and to suppress 3.4 GHz signal which back from output of the amplifier by a LPF structure in Fig. 6. Also output matching circuit is designed to amplify 2.4 GHz and 6.8 GHz output combined with the microstrip DGS.

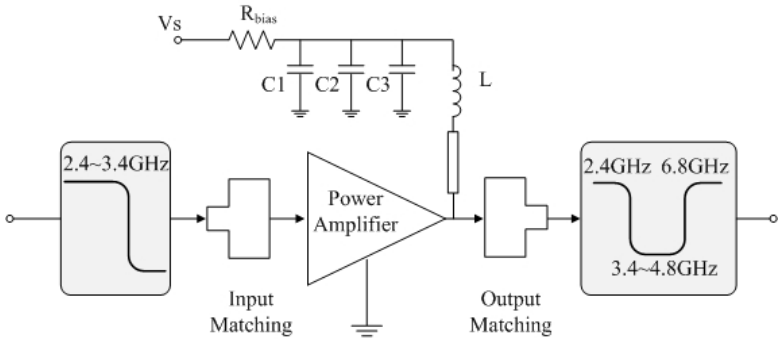

Figure 6. The proposed power amplifier with matching network.

As the advantages of DGS mentioned above, the proposed dual band module has a stopband characteristic to suppress the fundamental power of the frequency doubler as well as the second harmonic of the amplifier. Two types stop band characteristics are simulated in Fig. 7. Compared with the $\lambda/4$ reflector, the amplifier mode with the DGS is -38.1 dBc, while the second harmonic suppression is -35.2 dBc.

3. RESULTS AND DISCUSSIONS

The proposed dual band transmitter was fabricated by using microstrip circuit with HITTITE HMC313 GaAs InGaP Heterojunction broadband MMIC. The substrate parameters are $\varepsilon_r = 3.48$, and $\tan\delta = 0.002$. The photograph of 2.4 GHz and 6.8 GHz transmitter is shown in Fig. 8.

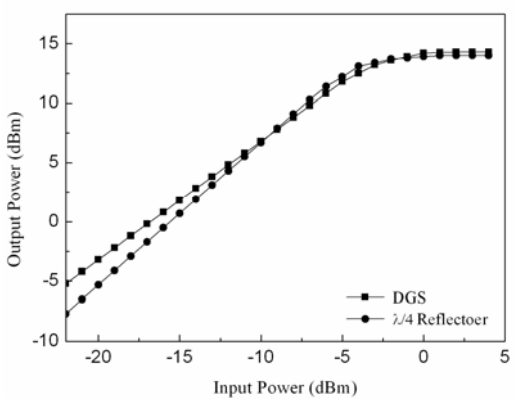

Figure 7. Simulated P_{in}–P_{out} characteristic of DGS and $\lambda/4$ reflector in amplifier mode.

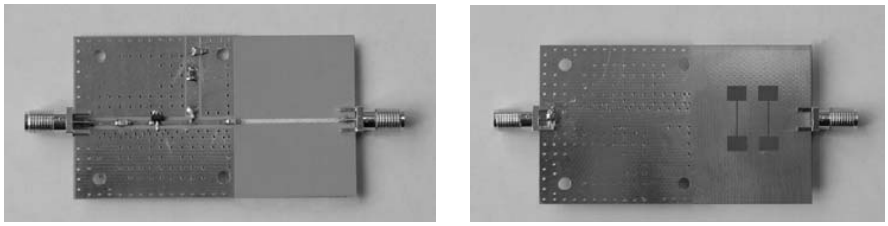

(a) Schematic top-view (b) Schematic ground-view

Figure 8. Photograph of the dualband transmitter (a) Schematic top-view, (b) Schematic ground-view.

Figure 9 shows the simulated results as well as the measured performances of the proposed DGS. Obviously, good agreement can be observed between the measured and simulated result, except that there is a little frequency shift at the second attenuation pole at 4.8 GHz. There are two transmission zeros which are important in practical applications on the stopband. They achieved −41.3 dB and −52.6 dB at the frequencies of 3.4 GHz and 4.8 GHz, respectively. The insertion loss at 2.4 GHz is about −0.132 dB by simulating while the measured results is about −0.152 dB at 2.4 GHz.

Figure 10 is the comparisons of the dual band module using DGS with $\lambda/4$ reflector. The measured results show that in the power amplifier model, the measured $P_{1\,dB}$ and the second harmonic suppression of DGS were improved by 0.9 dB and 22 dB, respectively.

Figure 11 shows the experimental results of fundamental power

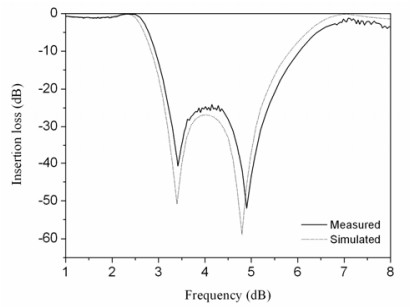

Figure 9. Simulated and measured results of the proposed DGS.

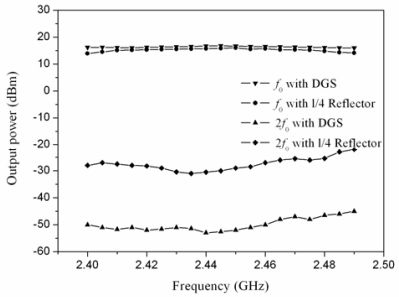

Figure 10. Comparison of $P_{1\,dB}$ and second harmonic with DGS and $\lambda/4$ reflector in amplifier mode.

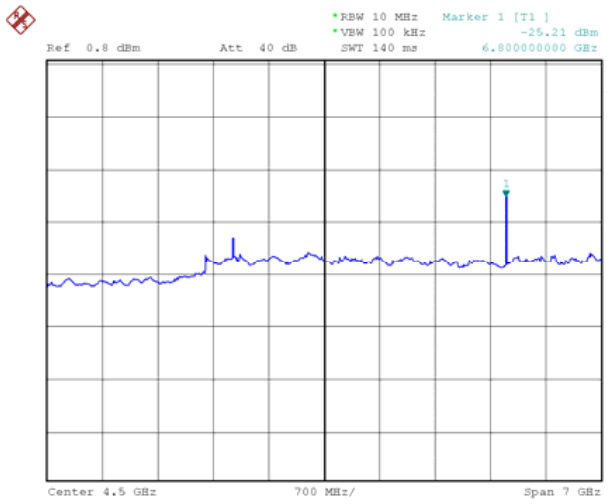

Figure 11. Output spectrum measured at 6.8 GHz in frequency doubler mode.

rejection in frequency doubler mode. When the fundamental input power is 0 dBm at 3.4 GHz, it is suppressed below −40 dBc and the output of second harmonic is about 4.5 dBm at 6.8 GHz. The maximum output power achieves 7.8 dBm in frequency doubler mode due to the input power amplified.

Figure 12 shows the measured results of the suppression with input power of 1 dBm at 2.4 GHz in power amplifier mode. As it is shown,

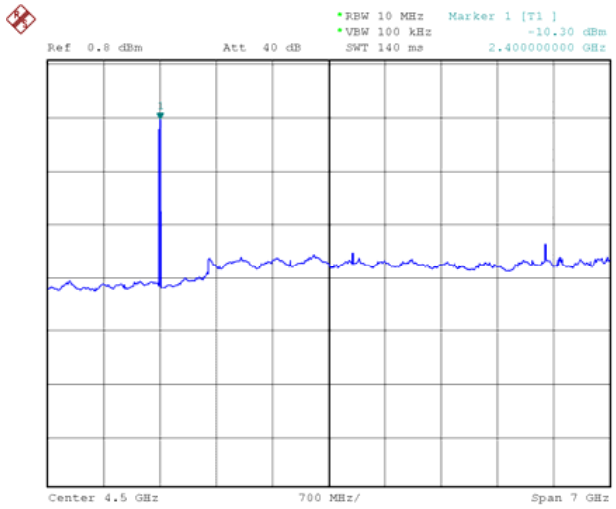

Figure 12. Output spectrum measured at 2.4 GHz in power amplifier mode.

the second harmonic is suppressed below −51 dBc. The gain of power amplifier is about 16.5 dB and its $P_{1\,dB}$ achieves 13.7 dBm.

4. CONCLUSION

The dual band module transmitter using the microstrip DGS is proposed and fabricated in this paper. By the stopband characteristics of proposed DGS from 3.4 GHz to 4.8 GHz, the second harmonic of the amplifier and fundamental power of the frequency doubler were suppressed. Compared with $\lambda/4$ reflector, the amplifier mode shows 22 dB improved suppression of the second harmonic, and the $P_{1\,dB}$ has 0.9 dB improvement with presented DGS. The $P_{1\,dB}$ and gain achieve 13.7 dBm and 16.5 dB at amplifier mode, and its maximum output power is 7.8 dBm at 6.8 GHz in frequency double mode. The implementation and performance measurement shows that the proposed DGS will be useful in the development of microstrip circuit design.

REFERENCES

1. Jeon, J. H., J. H. Choi, S. M. Kang, T. Y. Kim, W. Choi, and K. H. Koo, "A novel dual band transmitter for WLAN 802.11a/g

applications," *IEEE MTT-S Int. Microwave Symp. Dig.*, Vol. 2, 1285–1288, 2004.

2. Zhang, P., L. Der, D. Guo, I. Sever, T. Bourdi, C. Lam, A. Zolfaghari, J. Chen, D. Gambetta, B. Cheng, S. Gowder, S. Hart, L. Huynh, T. Nguyen, and B. Razavi, "A single-chip dual-band direct-conversion IEEE 802.11a/b/g WLAN transceiver in 0.18-µm CMOS," *IEEE J. Solid State Circuits*, Vol. 40, 1932–1937, 2005.
3. Xu, Z., S. Jiang, Y. Wu, H.-Y. Jian, G. Chu, K. Ku, P. Wang, N. Tran, Q. Gu, M.-Z. Lai, C. Chien, M. F. Chang, and P. D. Chow, "A compact dual-band direct-conversion CMOS transceiver for 802.11a/b/g wlan," *Dig. Tech. Pap. IEEE Int. Solid State Circuits Conf.*, Vol. 48, 68–69, 2005.
4. Kang, S. M., S. W. Nam, and K. H. Koo, "Adaptive linearization of frequency doubler using DGS," *IEEE MTT-S Int. Microwave Symp. Dig.*, 1225–1228, 2007.
5. Klepser, B.-U., M. Punzenberger, T. Ruhlicke, and M. Zannoth, "5-GHz and 2.4-GHz dual-band RF-transceiver for WLAN 802.11a/b/g applications," *IEEE Radio Freq. Integrated Circuits Symp. RFIC Dig. Tech. Pap.*, 37–40, 2003.
6. Deng, J., M. Chew, S. Vora, M. Cassia, T. Marra, K. Sahota, and V. Aparin, "A dual-band high efficiency CMOS transmitter for wireless CDMA applications," *IEEE Radio Freq. Integrated Circuits Symp.*, 25–28, 2007.
7. Park, Y., R. Melville, R. C. Frye, M. Chen, and J. S. Kenney, "Dual-band transmitters using digitally predistorted frequency multipliers for software defined radios," *IEEE MTT-S Int. Microwave Symp. Dig.*, Vol. 2, 547–550, 2004.
8. Zhao, L.-P., X. Zhai, B. Wu, T. Su, W. Xue, and C.-H. Liang, "Novel design of dual-mode bandpass filter using rectangle structure," *Progress In Electromagnetics Research B*, Vol. 3, 131–141, 2008.
9. Ghorbaninejad, H. and M. Khalaj-Amirhosseini, "Compact bandpass filters utilizing dielectric filled waveguides," *Progress In Electromagnetics Research B*, Vol. 7, 105–115, 2008.
10. Wang, X.-H., B.-Z. Wang, and K. J. Chen, "Compact broadband dual-band bandpass filters using slotted ground structures," *Progress In Electromagnetics Research*, PIER 82, 151–166, 2008.
11. Srivastava, R., K. B. Thapa, S. Pati, and S. P. Ojha, "Design of photonic band gap filter," *Progress In Electromagnetics Research*, PIER 81, 225–235, 2008.

12. Wu, G.-L., W. Mu, X.-W. Dai, and Y.-C. Jiao, "Design of novel dual-band bandpass filter with microstrip meander-loop resonator and CSRR DGS," *Progress In Electromagnetics Research*, PIER 78, 17–24, 2008.
13. Naghshvarian-Jahromi, M. and M. Tayarani, "Miniature planar UWB bandpass filters with circular slots in ground," *Progress In Electromagnetics Research Letters*, Vol. 3, 87–93, 2008.
14. Xiao, J.-K., "Triangular resonator bandpass filter with tunable operation," *Progress In Electromagnetics Research Letters*, Vol. 2, 167–176, 2008.
15. Choi, H.-J., J.-S. Lim, and Y.-C. Jeong, "A new design of Doherty amplifiers using defected ground structure," *IEEE Microwave Compon. Lett.*, Vol. 16, 687–689, 2006.
16. Wang, X.-H., B.-Z. Wang, H. Zhang, and K. J. Chen, "A tunable bandstop resonator based on a compact slotted ground structure," *IEEE Trans. Microwave Theory Tech.*, Vol. 55, 1912–1917, 2007.
17. Xiao, J. K., S. W. Ma, S. Zhang, and Y. Li, "Novel compact split ring stepped-impedance resonator (SIR) bandpass filters with transmission zeros," *Journal of Electromagnetic Waves and Applications*, Vol. 21, 329–339, 2007.
18. Xiao, J. K. and Y. Li, "Novel compact microstrip square ring bandpass filters," *Journal of Electromagnetic Waves and Applications*, Vol. 20, 1817–1826, 2006.
19. Wu, B., B. Li, T. Su, and C. H. Liang, "Equivalent-circuit analysis and lowpass filter design of split-ring resonator DGS," *Journal of Electromagnetic Waves and Applications*, Vol. 20, 1943–1953, 2006.
20. Youngcheol, P., R. Melville, R. C. Frye, A. M. C. Min Chen, and J. S. A. K. J. S. Kenney, "Dual-band transmitters using digitally predistorted frequency multipliers for reconfigurable radios," *IEEE Trans. Microwave Theory Tech.*, Vol. 53, 115–122, 2005.